



CHORUS

This is the accepted manuscript made available via CHORUS. The article has been published as:

## New Primary Mechanisms for the Synthesis of Rare $^9\text{Be}$ in Early Supernovae

Projjwal Banerjee, Yong-Zhong Qian, W. C. Haxton, and Alexander Heger

Phys. Rev. Lett. **110**, 141101 — Published 1 April 2013

DOI: [10.1103/PhysRevLett.110.141101](https://doi.org/10.1103/PhysRevLett.110.141101)

# New Primary Mechanisms for the Synthesis of Rare ${}^9\text{Be}$ in Early Supernovae

Projjwal Banerjee,<sup>1,\*</sup> Yong-Zhong Qian,<sup>2,†</sup> W. C. Haxton,<sup>1,‡</sup> and Alexander Heger<sup>3,§</sup>

<sup>1</sup>*Department of Physics, University of California,  
and Lawrence Berkeley National Laboratory, Berkeley, CA 94720*

<sup>2</sup>*School of Physics and Astronomy, University of Minnesota, Minneapolis, MN 55455*

<sup>3</sup>*Monash Centre for Astrophysics, School of Mathematical Sciences, Monash University, VIC 3800, Australia*

We present two new primary mechanisms for the synthesis of the rare nucleus  ${}^9\text{Be}$ , both triggered by  $\nu$ -induced production of  ${}^3\text{H}$  followed by  ${}^4\text{He}({}^3\text{H}, \gamma){}^7\text{Li}$  in the He shells of core-collapse supernovae. For progenitors of  $\sim 8 M_\odot$ ,  ${}^7\text{Li}({}^3\text{H}, n_0){}^9\text{Be}$  occurs during the rapid expansion of the shocked He shell. Alternatively, for ultra-metal-poor progenitors of  $\sim 11\text{--}15 M_\odot$ ,  ${}^7\text{Li}(n, \gamma){}^8\text{Li}(n, \gamma){}^9\text{Li}(e^- \bar{\nu}_e){}^9\text{Be}$  occurs with neutrons produced by  ${}^4\text{He}(\bar{\nu}_e, e^+ n){}^3\text{H}$ , assuming a hard effective  $\bar{\nu}_e$  spectrum from oscillations (which also leads to heavy element production through rapid neutron capture) and a weak explosion (so the  ${}^9\text{Be}$  survives shock passage). We discuss the associated production of  ${}^7\text{Li}$  and  ${}^{11}\text{B}$ , noting patterns in LiBeB production that might distinguish the new mechanisms from others.

PACS numbers: 26.30.Jk, 98.35.Bd, 97.60.Bw, 97.10.Tk

It was argued four decades ago that interactions between Galactic cosmic rays (GCRs) and nuclei in the interstellar medium (ISM) could approximately account for the abundances of  ${}^6,{}^7\text{Li}$ ,  ${}^9\text{Be}$ , and  ${}^{10,11}\text{B}$  observed in the present Galaxy [1]. The rarest of these isotopes,  ${}^9\text{Be}$  has been regarded as special. While big bang nucleosynthesis (BBN) produced an initial abundance of  ${}^7\text{Li}$  [2] and the  $\nu$  process in core-collapse supernovae (CCSNe) may account for much of the Galaxy’s current inventory of  ${}^7\text{Li}$  and  ${}^{11}\text{B}$  and some fraction of its  ${}^{10}\text{B}$  [3], it is widely accepted that  ${}^9\text{Be}$  is produced almost exclusively in the ISM by GCRs (e.g., [4]). In this regard, high-velocity ejecta from very energetic CCSNe can be considered similar to GCRs, though these events may be too rare to generate significant amounts of  ${}^9\text{Be}$  in the ISM [5]. Recent observations (e.g., [6]) show that there is a linear correlation between  $\log(\text{Be}/\text{H})$  and  $\log(\text{E}/\text{H})$  with a slope  $\sim 0.9\text{--}1$  over  $\sim 3$  dex, where E stands for O, Mg, Ti, and Fe, all of which are major primary products of CCSNe. While GCRs could produce such a correlation [4], the data motivated our search for alternative CCSN mechanisms for primary  ${}^9\text{Be}$  production. Primary mechanisms operating at low metallicities are potentially observable because their signatures would be preserved in local chemical enrichments influenced by just a few early CCSNe.

Here we describe two new primary mechanisms for the synthesis of  ${}^9\text{Be}$ , both occurring in the He shells of early CCSNe and driven by interactions of the  $\nu$ s from the central proto-neutron star (PNS). We calculate this nucleosynthesis with the hydrodynamic code KEPLER [7] using the most recent models of ultra-metal-poor massive progenitors evolved with this code. For a progenitor of  $8.1 M_\odot$ , the He shell, initially at a radius  $r \sim 10^9$  cm, is

exposed to an intense flux of  $\nu$ s during its expansion following shock passage. Production of  ${}^9\text{Be}$  occurs through  ${}^4\text{He}({}^3\text{H}, \gamma){}^7\text{Li}({}^3\text{H}, n_0){}^9\text{Be}$  with  ${}^3\text{H}$  made by  $\nu$  reactions on  ${}^4\text{He}$ . For progenitors of 11 and  $15 M_\odot$ , the reaction  ${}^4\text{He}(\bar{\nu}_e, e^+ n){}^3\text{H}$  in their outer He shells at  $r \sim 10^{10}$  cm can produce sufficient neutron densities to drive both a rapid ( $r$ ) neutron-capture process, as described recently in [8], and a correlated “mini- $r$  process” in which  ${}^7\text{Li}$  is converted to  ${}^9\text{Be}$ . We explore the sensitivities of the  ${}^9\text{Be}$  yields, as well as the associated  $\nu$ -process yields of  ${}^7\text{Li}$  and  ${}^{11}\text{B}$ , to  $\nu$  emission spectra, flavor oscillations, and the explosion energy. We discuss the implications for observations at low metallicities and consider other mechanisms for  ${}^9\text{Be}$  production at higher metallicities.

In the updated version of KEPLER, a full reaction network is used to evolve the nuclear composition of a massive star throughout its lifetime and to follow the nucleosynthesis that accompanies the explosion. This includes the nucleosynthesis associated with shock heating of the star’s mantle and  $\nu$ -process nucleosynthesis associated with a  $\nu$  burst carrying  $\sim 300$  B (“Bethe”;  $1 \text{ B} = 10^{51}$  ergs). All  $\nu$  reactions on  ${}^4\text{He}$  are included as in [8]. The KEPLER progenitors employed here, denoted by u8.1, u11, and u15, have initial metallicities (total mass fraction of elements heavier than He) of  $Z = 10^{-4} Z_\odot$  and masses of  $8.1$ ,  $11$ , and  $15 M_\odot$  [9]. These models are very similar to earlier ones evolved with a more limited reaction network [10]. The three selected stars develop Fe cores by the end of their evolutions. We simulate an explosion by driving a piston into the collapsing progenitor and following the propagation of the resulting shock wave [7]. Consistent with  $\nu$  transport calculations and  $\nu$  signals from SN 1987A, we assume that the PNS cools by  $\nu$  emission according to  $L_\nu(t) = L_\nu(0) \exp(-t/\tau_\nu)$ , with an initial luminosity per species of  $L_\nu(0) = 16.7 \text{ B/s}$  and time constant  $\tau_\nu = 3$  s, where  $t = 0$  marks the launching of the piston. The  $\nu$  spectra are approximated as Fermi-Dirac distributions with zero chemical potential and fixed temperatures  $T_{\nu_e}$ ,  $T_{\bar{\nu}_e}$ , and  $T_{\nu_x} = T_{\bar{\nu}_x}$  ( $x = \mu, \tau$ ).

A large set of calculations was performed to assess

---

\*Electronic address: [projjwal@berkeley.edu](mailto:projjwal@berkeley.edu)

†Electronic address: [qian@physics.umn.edu](mailto:qian@physics.umn.edu)

‡Electronic address: [haxton@berkeley.edu](mailto:haxton@berkeley.edu)

§Electronic address: [alexander.heger@monash.edu](mailto:alexander.heger@monash.edu)

the sensitivity of the nucleosynthesis to the explosion energy,  $\nu$  spectra, and flavor oscillations. CCSN simulations using progenitors similar to u8.1 produce weak explosions with energies of  $E_{\text{expl}} \lesssim 0.1$  B [11], while observations suggest  $E_{\text{expl}} \sim 1$  B for more massive progenitors of  $\sim 13\text{--}20 M_{\odot}$  (Fig. 1 of [12]). Below we discuss results for  $E_{\text{expl}} \sim 0.06\text{--}0.3$  B (u8.1) and  $0.1\text{--}1$  B (u11/u15). Two sets of  $\nu$  temperatures were used:  $(T_{\nu_e}, T_{\bar{\nu}_e}, T_{\nu_x}) = (4, 5.33, 8)$  MeV (H) and  $(3, 4, 6)$  MeV (S), which represent the harder and softer spectra obtained from earlier (e.g., [13]) and more recent [14]  $\nu$  transport calculations, respectively. For an inverted  $\nu$  mass hierarchy,  $\bar{\nu}_e \leftrightarrow \bar{\nu}_x$  oscillations occur before  $\nu$ s reach the He shell, which greatly increases the rate of  ${}^4\text{He}(\bar{\nu}_e, e^+n){}^3\text{H}$  [8]. We will explore the case of full  $\bar{\nu}_e \leftrightarrow \bar{\nu}_x$  interconversion. We label the nucleosynthesis calculations by the progenitor model, the  $\nu$  spectra, and the explosion energy in units of B, with, e.g., u8.1H.1 indicating progenitor model u8.1, the harder  $\nu$  spectra H, and  $E_{\text{expl}} = 0.1$  B. Calculations including  $\bar{\nu}_e \leftrightarrow \bar{\nu}_x$  oscillations are denoted by a bar above the H or S. The abundances of  ${}^{28}\text{Si}$  and  ${}^{32}\text{S}$  in the He shells of u11 and u15 are  $\sim 10\text{--}30$  times larger than those found in the older models of [10]. Consequently, we also considered modified models u11\* and u15\* in which the He-shell abundances of  ${}^{28}\text{Si}$  and  ${}^{32}\text{S}$  were reduced to their former values. Representative total mass yields of  ${}^9\text{Be}$ ,  ${}^7\text{Li}$ ,  ${}^{11}\text{B}$ , and Fe are given in Table I.

TABLE I: Yields of  ${}^9\text{Be}$ ,  ${}^7\text{Li}$ ,  ${}^{11}\text{B}$ , and Fe in  $M_{\odot}$

model	${}^9\text{Be}$	${}^7\text{Li}$	${}^{11}\text{B}$	Fe
u8.1 $\bar{\text{H}}$ .06	1.57(−10)	2.77(−7)	1.47(−7)	1.89(−3)
u8.1 $\bar{\text{H}}$ .1	1.97(−10)	2.97(−7)	1.35(−7)	1.75(−3)
u8.1H.1	1.20(−10)	2.47(−7)	1.34(−7)	1.79(−3)
u8.1 $\bar{\text{S}}$ .1	5.02(−11)	1.11(−7)	5.67(−8)	1.79(−3)
u8.1S.1	2.55(−11)	8.19(−8)	5.05(−8)	1.80(−3)
u8.1 $\bar{\text{H}}$ .3	2.56(−10)	3.03(−7)	1.06(−7)	1.45(−3)
u11 $\bar{\text{H}}$ .1	1.43(−9)	2.0–2.3(−7)	2.2–8.7(−7)	< 7.73(−2)
u11* $\bar{\text{H}}$ .1	9.14(−9)	1.5–1.9(−7)	2.6–9.5(−7)	< 7.68(−2)
u11* $\bar{\text{H}}$ .3	9.81(−10)	3.26(−7)	1.09(−6)	< 8.75(−2)
u15 $\bar{\text{H}}$ .1	< 5.20(−10)	< 3.33(−7)	< 1.34(−6)	< 4.42(−2)
u15* $\bar{\text{H}}$ .1	< 2.92(−9)	< 3.15(−7)	< 1.36(−6)	< 4.42(−2)
u15* $\bar{\text{H}}$ .3	7.21(−10)	1.69(−7)	9.50(−7)	< 4.62(−2)

Note:  $X(Y) \equiv X \times 10^Y$

Progenitors of  $\sim 8 M_{\odot}$  have a steeply-falling density profile outside the core and He-shell radii  $r \sim 10^9$  cm, in contrast to  $\sim 10^{10}$  cm for progenitors of  $\gtrsim 11 M_{\odot}$ . We use Zone 95 in u8.1 $\bar{\text{H}}$ .1 to illustrate  ${}^9\text{Be}$  production in such progenitors. Prior to shock arrival, the radius, temperature, and density of this zone are  $1.58 \times 10^9$  cm,  $2.21 \times 10^8$  K, and  $279 \text{ g/cm}^3$ , respectively. The three most abundant nuclei are  ${}^4\text{He}$ ,  ${}^{12}\text{C}$ , and  ${}^{16}\text{O}$  with initial mass fractions of 0.948, 0.043, and 0.009, respectively. The time evolution of the number fraction  $Y_i$  for various nuclei is shown in Fig. 1. Upon being shocked at  $t \sim 0.7$  s, Zone 95 reaches a peak temperature of  $\sim 8 \times 10^8$  K, so that any  ${}^9\text{Be}$  produced previously is burned up. By

$t \sim 5$  s the shocked material has expanded and cooled to  $\sim 2 \times 10^8$  K, effectively turning off the principal destruction reactions  ${}^9\text{Be}(p, {}^4\text{He}){}^6\text{Li}$  and  ${}^9\text{Be}(p, d)2{}^4\text{He}$ . Yet as the material is still close to the PNS and the time still relatively early in units of  $\tau_{\nu}$ , the flux of  $\nu$ s can efficiently drive the breakup reactions  ${}^4\text{He}(\nu, \nu'n){}^3\text{He}$ ,  ${}^4\text{He}(\nu, \nu'p){}^3\text{H}$ , and  ${}^4\text{He}(\bar{\nu}_e, e^+n){}^3\text{H}$ . Production of  ${}^9\text{Be}$  occurs through  ${}^4\text{He}({}^3\text{H}, \gamma){}^7\text{Li}({}^3\text{H}, n_0){}^9\text{Be}$ . Note that  ${}^9\text{Be}$  must be produced in the ground state (hence  $n_0$ ) because all of its excited states are unstable to breakup. We took the rate for  ${}^7\text{Li}({}^3\text{H}, n_0){}^9\text{Be}$  from [15].

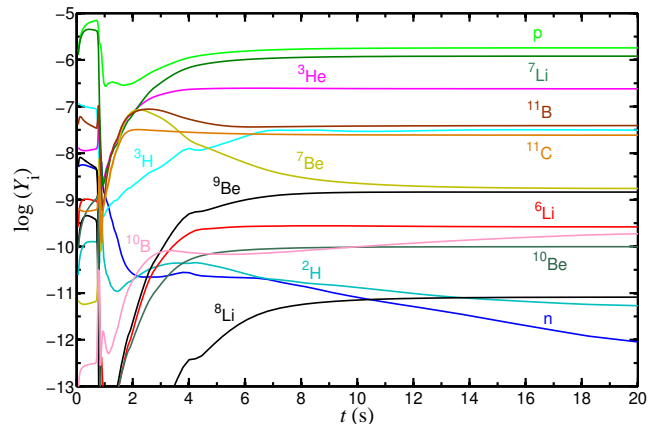


FIG. 1: Time evolution of the number fraction  $Y_i$  for various nuclei in Zone 95, a typical zone producing  ${}^9\text{Be}$  in u8.1 $\bar{\text{H}}$ .1.

The yield of  ${}^9\text{Be}$  decreases by a factor of  $\sim 4$  from u8.1 $\bar{\text{H}}$ .1 to u8.1 $\bar{\text{S}}$ .1 (Table I). This reflects the high thresholds of the breakup reactions  ${}^4\text{He}(\nu, \nu'p){}^3\text{H}$  and  ${}^4\text{He}(\bar{\nu}_e, e^+n){}^3\text{H}$ , and consequently, their sensitivity to the high-energy tails of the  $\nu$  spectra. The presence of neutral-current production of  ${}^3\text{H}$  reduces the sensitivity to  $\bar{\nu}_e \leftrightarrow \bar{\nu}_x$  oscillations: other factors being the same, oscillations increase the yield by up to a factor of  $\sim 2$ . We also explored different explosion energies based on current CCSN models [11]. The change from u8.1 $\bar{\text{H}}$ .1 to u8.1 $\bar{\text{H}}$ .06 (u8.1 $\bar{\text{H}}$ .3) produces a 20% decrease (30% increase) in the  ${}^9\text{Be}$  yield primarily through the expansion rate of the shocked He-shell material: a higher  $E_{\text{expl}}$  results in faster cooling to  $\sim 2 \times 10^8$  K and hence, more  ${}^9\text{Be}$ . The  ${}^9\text{Be}$  production in progenitors like u8.1 depends on the sharply-falling density structure outside the core: the He shell is shocked, expands, and cools on timescales comparable to  $\tau_{\nu}$ , and thus before the  $\nu$  flux has diminished significantly. In such progenitors the yield is essentially independent of the initial metallicity.

As in the u8.1 models, any  ${}^9\text{Be}$  produced prior to shock arrival in the inner He shells of the u11/u15 models is destroyed by shock heating. The subsequent  $\nu$ -induced replenishment of  ${}^3\text{H}$  and thus  ${}^7\text{Li}$  that leads to  ${}^9\text{Be}$  production in the rapidly expanding and cooling He-shell ejecta of the u8.1 models is not replicated in the u11/u15 models, due to the much smaller  $\nu$  fluxes associated with the latter's much larger He-shell radii and longer delay

in shock arrival there. Instead, the synthesis of  ${}^9\text{Be}$  in these models depends on its preshock buildup in outer He shells and its postshock survival due to diminished shock heating there.

We illustrate this mechanism in u11\* $\overline{\text{H.1}}$ , which is very similar to the model recently used in [8] to demonstrate a  $\nu$ -induced  $r$ -process in outer He shells at low metallicities (modifying scenarios discussed earlier in [3, 16]). As in [8], we make use of  ${}^4\text{He}(\bar{\nu}_e, e^+){}^3\text{H}$  as an important neutron source that can be enhanced by  $\bar{\nu}_e \leftrightarrow \bar{\nu}_x$  oscillations. Zone 223 is representative of  ${}^9\text{Be}$  production in u11\* $\overline{\text{H.1}}$ . Prior to shock arrival, its radius, temperature, and density are  $1.10 \times 10^{10}$  cm,  $8.49 \times 10^7$  K, and  $50$  g/cm $^3$ . The composition is nearly pure  ${}^4\text{He}$ , with initial mass fractions of  $\sim 10^{-5}$ ,  $10^{-8}$ ,  $4 \times 10^{-9}$ , and  $4 \times 10^{-8}$  for  ${}^{12}\text{C}$ ,  ${}^{28}\text{Si}$ ,  ${}^{32}\text{S}$ , and  ${}^{56}\text{Fe}$ , respectively. Figure 2 shows the time evolution of  $Y_i$  for important nuclei.

We find that the above neutron source drives both the  $r$ -process described in [8] and an analogous “mini- $r$  process” through  ${}^7\text{Li}(n, \gamma){}^8\text{Li}(n, \gamma){}^9\text{Li}(e^- \bar{\nu}_e){}^9\text{Be}$ . The  ${}^9\text{Be}$  yield is limited by the short 838 ms half-life of  ${}^8\text{Li}$ , which  $\beta$  decays through the 3.0 MeV resonance in  ${}^8\text{Be}$  to  ${}^4\text{He} + {}^4\text{He}$ , and by the 49.5% branching ratio for  ${}^9\text{Li}$  to decay to particle-unstable excited states in  ${}^9\text{Be}$ . The “mini- $r$  process” operates for  $\sim 20$  s prior to shock arrival, at which time the temperature and density jump to  $\sim 2 \times 10^8$  K and  $\sim 220$  g/cm $^3$ , respectively, and a short burst of neutrons is released by  ${}^8\text{Li}({}^4\text{He}, n){}^{11}\text{B}$  (Fig. 2). Incomplete destruction of  ${}^9\text{Be}$  occurs during the few seconds in which the postshock temperature stays at  $\sim 2 \times 10^8$  K, as protons generated by  ${}^4\text{He}(\nu, \nu'){}^3\text{H}$  are consumed by  ${}^9\text{Be}(p, {}^4\text{He}){}^6\text{Li}$  and  ${}^9\text{Be}(p, d){}^2{}^4\text{He}$  (Fig. 2).

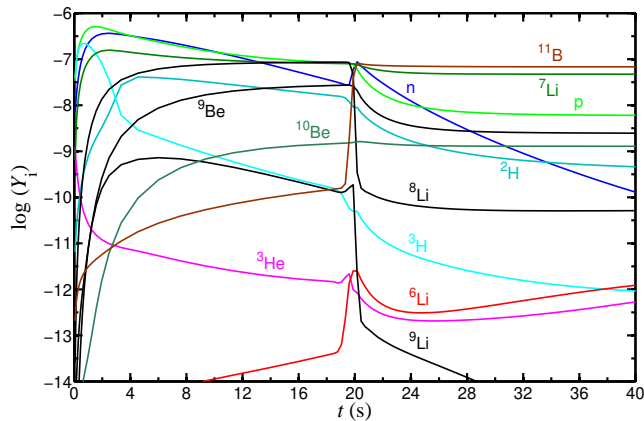


FIG. 2: Time evolution of the number fraction  $Y_i$  for various nuclei in Zone 223, a typical zone producing  ${}^9\text{Be}$  in u11\* $\overline{\text{H.1}}$ .

The production of  ${}^9\text{Be}$  in the u11/u15 models is sensitive to the explosion energy (Table I). The higher postshock temperatures found in more energetic explosions greatly enhance  ${}^9\text{Be}$  destruction. For  $E_{\text{expl}} \gtrsim 1$  B, essentially all of the  ${}^9\text{Be}$  made in the He shell prior to shock arrival is destroyed: only that produced in the oxygen shell through  ${}^{12}\text{C}(\nu, \nu'){}^3\text{He} + {}^9\text{Be}$  [3] survives. The absence

of protons and  ${}^4\text{He}$  in the oxygen shell eliminates light-particle reactions through which  ${}^9\text{Be}$  can be destroyed.

The  ${}^9\text{Be}$  yields for the u11/u15 models are also sensitive to the He-shell composition (Table I). The abundances of the hydrostatic-burning products  ${}^{28}\text{Si}$  and  ${}^{32}\text{S}$  are  $\sim 10$ – $30$  times higher in u11/u15 than in u11\*/u15\*. As  ${}^{28}\text{Si}$  and  ${}^{32}\text{S}$  are neutron sinks,  $Y_n$  is consequently reduced in u11/u15. The effects on  ${}^9\text{Be}$  yields are quadratic in  $Y_n$ , as two neutrons are captured to produce  ${}^9\text{Be}$ . Increasing the initial metallicity also reduces  $Y_n$  due to neutron sinks such as  ${}^{56}\text{Fe}$ . He-shell production of  ${}^9\text{Be}$  dominates oxygen-shell production only for initial metallicities of  $Z \lesssim 10^{-3} Z_{\odot}$ . A similar bound on He-shell metallicity comes from requiring a neutron density capable of supporting a  $\nu$ -induced  $r$ -process [8]. As for this process,  ${}^9\text{Be}$  synthesis requires both hard  $\nu$  spectra and  $\bar{\nu}_e \leftrightarrow \bar{\nu}_x$  oscillations characteristic of an inverted mass hierarchy so that  $\nu$  reactions can produce an adequate  $Y_n$ .

In summary,  ${}^9\text{Be}$  synthesis in the He zones of models like u11/u15 requires an accompanying  $r$ -process and  $E_{\text{expl}} \lesssim 0.3$  B. Severe fallback of inner layers was found to occur in all u11/u15 models with  $E_{\text{expl}} \lesssim 0.3$  B. Table I thus only gives ranges or upper limits for the yields when production partially or entirely occurs in the fallback zones. The actual yields in these cases depend on the extent of the poorly-understood mixing and ejection associated with fallback.

In the models we explored,  ${}^9\text{Be}$  production is accompanied by production of  ${}^7\text{Li}$  and  ${}^{11}\text{B}$  (Table I). In all u11/u15 models the latter production operates as described in [3], through  $\nu$  breakup of  ${}^4\text{He}$  and  ${}^{12}\text{C}$  prior to shock arrival. In contrast, large fractions of  ${}^7\text{Li}$  and  ${}^{11}\text{B}$  are produced in u8.1 models by  $\nu$  interactions occurring in the O-Ne shell that has been severely altered by shock passage. Because this shell is so close ( $r \sim 1.8 \times 10^8$  cm) to the core, shock passage leads to complete disassociation of nuclei, which then are reassembled into  ${}^4\text{He}$  and Fe-group nuclei as the shell expands and cools. The  $\nu$  irradiation of this material leads to  ${}^4\text{He}({}^3\text{He}, \gamma){}^7\text{Be}({}^4\text{He}, \gamma){}^{11}\text{C}$ . The subsequent decay of  ${}^7\text{Be}$  and  ${}^{11}\text{C}$  accounts for, e.g.,  $\sim 70\%$  of the  ${}^7\text{Li}$  and  $\sim 43\%$  of the  ${}^{11}\text{B}$  produced in u8.1 $\overline{\text{H.1}}$ . Properties of  ${}^7\text{Li}$  and  ${}^{11}\text{B}$  production in all u8.1 models studied include: 1) weak dependence on  $\nu$  spectra, flavor oscillations, and the explosion energy and no fallback; 2) stable yields within a factor of  $\sim 2$  of  $1.6 \times 10^{-7}$  and  $8.6 \times 10^{-8} M_{\odot}$ , respectively; 3) a number-yield ratio  ${}^{11}\text{B}/{}^7\text{Li}$  of  $\sim 0.2$ – $0.4$ , comparable to the solar value of 0.29 [17] and distinct from the values of  $\sim 1$ – $3.6$  found in u11/u15 models. The last point is of interest because in the more massive progenitors  ${}^{11}\text{B}$  tends to overwhelm all other yields [3, 18]. For all the models in Table I, production of  ${}^6\text{Li}$  and  ${}^{10}\text{B}$  is negligible with  ${}^6\text{Li}/{}^7\text{Li} \lesssim 10^{-4}$  and  ${}^{10}\text{B}/{}^{11}\text{B} \sim (0.5\text{--}2) \times 10^{-2}$ .

Proposed mechanisms for Be production can be tested against observations. The GCR mechanism (e.g., [4]) is severely constrained by a recent study [6] showing that  $[\text{Be}/\text{Fe}] \equiv \log(\text{Be}/\text{Fe}) - \log(\text{Be}/\text{Fe})_{\odot} \sim 0 \pm 0.5$  for a large sample of stars covering  $[\text{Fe}/\text{H}] \sim -3.5$  to  $-0.5$ . Using



the yields in Table I and the solar abundances in [17], one obtains  $[\text{Be}/\text{Fe}] \sim 0 \pm 0.2$  for at least three cases: (I) all the u8.1 models with the hard  $\nu$  emission spectra, (II) u11\* $\overline{\text{H}}$ .1 with the maximum possible Fe yield, and (III) u11 $\overline{\text{H}}$ .1, u11\* $\overline{\text{H}}$ .3, and u15\* $\overline{\text{H}}$ .3 if their actual Fe yields are  $\sim 10\%$  of the upper limits.

At metallicities for which the ISM was enriched mostly by a single CCSN, yields would be mixed with a total mass of hydrogen of  $\sim 10^3 (E_{\text{expl}}/0.1 \text{ B})^{6/7} M_{\odot}$  [19]. One finds  $[\text{Fe}/\text{H}] \sim -3.5$  to  $-2.8$  (I),  $-1.4$  (II), and  $-3$  to  $-2.4$  (III) for the above cases. The corresponding enrichment of Li is  $A(\text{Li}) \equiv \log(\text{Li}/\text{H}) + 12 \sim 1-1.8$ . This is well below the level due to BBN and thus consistent with the plateau  $A(\text{Li}) \sim 2.2$  observed at these metallicities [2]. Our models also give  $A(\text{B}) \sim 0.6-1.3$ ,  $1.4-1.9$ , and  $1.3-1.9$  with  $\text{B}/\text{Be} \sim (3-9) \times 10^2$ ,  $20-85$ , and  $10^2-10^3$  in Cases I, II, and III, respectively. The limited data on B at  $[\text{Fe}/\text{H}] \leq -1.4$  show  $A(\text{B}) \sim 0-1.8$  but typically with rather low  $\text{B}/\text{Be}$  values of  $\sim 10-20$  [20]. Large  $\text{B}/\text{Be}$  values have been observed but are usually attributed to greater depletion of Be relative to B in stars [20]. Simultaneous observations of Be and B carried out for more stars at  $[\text{Fe}/\text{H}] \leq -1.4$  could test this interpretation, versus the intrinsic high yield ratio of  $\text{B}/\text{Be}$  for our models.

While our u8.1 mechanism continues to operate with increasing metallicity, the mass range of candidate progenitors is likely to shrink [10], limiting their integrated contribution to the Galactic inventory of  ${}^9\text{Be}$ . Indeed, the low solar value of  $\text{B}/\text{Be} \approx 31$  [17] requires other  ${}^9\text{Be}$  production mechanisms, e.g., those accompanying the  $r$ -

process in recent simulations of neutron star (NS) mergers [21]. Thus we regard both of the new mechanisms discussed here as low-metallicity, candidate primary processes that could naturally explain the linear growth of  ${}^9\text{Be}$  with CCSN-associated metals at  $[\text{Fe}/\text{H}] \lesssim -1.4$ .

In conclusion, we stress that candidate processes for early  ${}^9\text{Be}$  production, including the two primary mechanisms described here as well as adaptations of the GCR mechanism, elevate the importance of observations to determine both overall trends in early LiBeB evolution and specific abundance patterns that may characterize local enrichments in these elements. The more exotic of our two mechanisms requires special conditions: hard  $\nu$  emission spectra,  $\bar{\nu}_e \leftrightarrow \bar{\nu}_x$  oscillations, low metallicities, and low explosion energies, the first three of which are also needed for a simultaneous  $\nu$ -driven  $r$ -process. The possible correlation of an early  $r$ -process with  ${}^9\text{Be}$  production may be a feature of these processes that observers could exploit. Finally, we note that the nuclear physics of the two mechanisms explored here is not exotic: the necessary conditions are likely to be found in other astrophysical sites, with NS [21] and white dwarf [22] mergers being obvious possibilities.

We thank S. Goriely and H.-T. Janka for sharing their results on NS mergers. This work was supported in part by the US DOE [DE-SC00046548 (Berkeley), DE-AC02-98CH10886 (LBL), and DE-FG02-87ER40328 (UM)]; by the NSF [PHY02-16783 (JINA)]; by ARC Future Fellowship FT120100363 (AH); and by the Alexander von Humboldt Foundation (WCH).

- 
- [1] H. Reeves, W. A. Fowler, and F. Hoyle, *Nature* **226**, 727 (1970); M. Meneguzzi, J. Audouze, and H. Reeves, *Astron. Astrophys.* **15**, 337 (1971).
- [2] See e.g., B. D. Fields, *Annu. Rev. Nucl. Part. Sci.* **61**, 47 (2011) for a review.
- [3] S. E. Woosley, D. H. Hartmann, R. D. Hoffman, and W. C. Haxton, *Astrophys. J.* **356**, 272 (1990).
- [4] N. Prantzos, *Astron. Astrophys.* **542**, A67 (2012). See also R. Ramaty, B. Kozlovsky, R. E. Lingenfelter, and H. Reeves, *Astrophys. J.* **488**, 730 (1997).
- [5] B. D. Fields, F. Daigne, M. Cassé, and E. Vangioni-Flam, *Astrophys. J.* **581**, 389 (2002); K. Nakamura, S. Inoue, S. Wanajo, and T. Shigeyama, *Astrophys. J.* **643**, L115 (2006).
- [6] A. M. Boesgaard, J. A. Rich, E. M. Levesque, and B. P. Bowler, *Astrophys. J.* **743**, 140 (2011).
- [7] T. A. Weaver, G. B. Zimmerman, and S. E. Woosley, *Astrophys. J.* **225**, 1021 (1978); T. Rauscher, A. Heger, R. D. Hoffman, and S. E. Woosley, *Nucl. Phys. A* **718**, 463 (2003).
- [8] P. Banerjee, W. C. Haxton, and Y.-Z. Qian, *Phys. Rev. Lett.* **106**, 201104 (2011).
- [9] A. Heger, S. E. Woosley, W. Zhang, and C. Joggerst, in preparation (2013).
- [10] S. E. Woosley, A. Heger, and T. A. Weaver, *Rev. Mod. Phys.* **74**, 1015 (2002).
- [11] F. S. Kitaura, H.-T. Janka, and W. Hillebrandt, *Astron. Astrophys.* **450**, 345 (2006).
- [12] N. Tominaga, H. Umeda, and K. Nomoto, *Astrophys. J.* **660**, 516 (2007).
- [13] S. E. Woosley, J. R. Wilson, G. J. Mathews, R. D. Hoffman, and B. S. Meyer, *Astrophys. J.* **433**, 229 (1994).
- [14] L. Hüdepohl *et al.*, *Phys. Rev. Lett.* **104**, 251101 (2010); T. Fischer *et al.*, *Astron. Astrophys.* **517**, A80 (2010).
- [15] C. R. Brune, R. W. Kavanagh, S. E. Kellogg, and T. R. Wang, *Phys. Rev. C* **43**, 875 (1991); A. Coc *et al.*, *Nucl. Phys. A* **538**, 515c (1992).
- [16] R. I. Epstein, S. A. Colgate, and W. C. Haxton, *Phys. Rev. Lett.* **61**, 2038 (1988); D. K. Nadyozhin, I. V. Panov, and S. I. Blinnikov, *Astron. Astrophys.* **335**, 207 (1998); D. K. Nadyozhin and I. V. Panov, *J. Phys. G* **35**, 014061 (2008).
- [17] K. Lodders, in *Principles and Perspectives in Cosmochemistry*, eds. A. Goswami and B. E. Reddy (Springer, Heidelberg, 2010) 379.
- [18] S. M. Austin, A. Heger, and C. Tur, *Phys. Rev. Lett.* **106**, 152501 (2011).
- [19] K. Thornton, M. Gaudlitz, H.-T. Janka, and M. Steinmetz, *Astrophys. J.* **500**, 95 (1998).
- [20] A. M. Boesgaard, E. J. McGrath, D. L. Lambert, and K. Cunha, *Astrophys. J.* **606**, 306 (2004); K. Tan, J. Shi, and G. Zhao, *Astrophys. J.* **713**, 458 (2010).
- [21] S. Goriely, A. Bauswein, and H.-T. Janka, *Astrophys. J.* **738**, L32 (2011).

- [22] K. J. Shen, L. Bildsten, D. Kasen, and E. Quataert, *Astrophys. J.* **748**, 35 (2012).